

Research Article

Kubra Telli and Ozden Yalcin-Ozuysal*

Epithelial-mesenchymal transition as a potential route for DAPT resistance in breast cancer cells

<https://doi.org/10.1515/tjb-2022-0218>

Received September 30, 2022; accepted November 21, 2022;

published online February 6, 2023



Abstract

Objectives: Notch is a conserved pathway involved in cell fate determination and homeostasis. Its dysregulation plays a role in poor prognosis and drug resistance in breast cancer. Targeting Notch signaling via inhibition of the gamma-secretase complex is in the spotlight of modern cancer treatments. Gamma-secretase inhibitors (GSI) have shown successful clinical activity in treating cancers, yet the possible resistance mechanism remains unstudied. Modeling the resistance and understanding culprit molecular mechanisms can improve GSI therapies. Accordingly, the aim of this study is to generate and analyze GSI-resistant breast cancer cells.

Methods: Gradually increasing doses of DAPT, a well-known GSI, were applied to MCF-7 breast cancer cell lines to generate resistance. Cell viability, migration and gene expressions were assessed by MTT, wound healing and qRT-PCR analyses.

Results: DAPT-resistant MCF-7 cells exhibited abnormal expression of Notch receptors, Notch targets (HES1, HES5, HEY1), and epithelial-mesenchymal transition (EMT) markers (E-cadherin, ZO-1, SNAIL2, N-cadherin) to overcome the continuous increase in DAPT toxicity by increased migration through mesenchymal transition.

Conclusions: This study prospects into the role of EMT in the potential resistance mechanism against DAPT treatment for breast cancer cells. Complementary targeting of EMT should be investigated further for a possible effect to potentiate DAPT's anti-cancer effects.

Keywords: breast cancer; DAPT; drug resistance; epithelial-mesenchymal transition; gamma secretase inhibitors; migration; notch signaling pathway.

Introduction

Cancer is a collection of diverse, dynamic, and complex neoplastic diseases that remains the cause of the highest mortality rate worldwide. Single or combinational drug treatments have been one of the most efficient ways to treat various cancers for over sixty years. Even so, there is still a problem faced in clinical oncology since cancer cells can show resistance to these therapies [1]. Resistance patterns against anti-neoplastic drugs are categorized into two; intrinsic and acquired. Intrinsic resistance is defined as the lack of initial toxic response per contra, acquired resistance is induced following the treatment, and both result in the failure of therapy. Approximately after six to twelve months of chemotherapy, 30% of breast cancer patients suffer from recurred cancer that becomes cross-resistant to multiple anti-neoplastic drugs [2]. Intracellular drug toxicity is reduced by various mechanisms, including overexpression of the ATP-Binding Cassette (ABC) transporter family, the establishment of a pro-tumorigenic microenvironment, and induction of epithelial-mesenchymal transition (EMT). Modulating signaling pathways play a crucial role in overturning the drug's effects. These pathways are targeted by novel therapeutic strategies to overcome drug resistance [1, 3].

Notch is a conserved signaling pathway involved in embryonic development, organogenesis, tissue homeostasis, cell proliferation, differentiation, and apoptosis regulation. There are five Notch ligands (Jagged 1, 2, Delta-like 1 (DLL1), 3, and 4) and four receptors (Notch 1, 2, 3, and 4) that interact non-covalently [4]. Ligand-receptor interaction induces cleavage of the receptors by the gamma-secretase complex (Presenilin, PEN2, APH1, and Nicastrin) to release the Notch intracellular domain (NICD). NICD then translocates into the nucleus to control gene expression. Notch signaling regulates various cellular processes such as apoptosis, drug

*Corresponding author: **Ozden Yalcin-Ozuysal**, Department of Molecular Biology and Genetics, Izmir Institute of Technology, 35430, Urla, İzmir, Türkiye, Phone: +90 232 750 7311, E-mail: ozdenyalcin@iyte.edu.tr. <https://orcid.org/0000-0003-0552-368X>

Kubra Telli, Department of Molecular Biology and Genetics, Izmir Institute of Technology, İzmir, Türkiye, E-mail: kubratelli@iyte.edu.tr. <https://orcid.org/0000-0003-2665-6289>

resistance, differentiation, proliferation, and cellular homeostasis via direct or indirect regulation of targets such as HES and HEY family of transcription factors, EMT regulators, cell cycle, and apoptosis-related factors [5]. Dysregulated Notch signaling results in aberrant expression of its downstream molecular targets and triggers anti- or pro-tumorigenic traits depending on the cell and tissue type. Notch signaling is aberrantly activated in breast cancer, behaving as an oncogene as it triggers breast tumorigenesis and correlates with poor prognosis and therapy resistance. Thus, several approaches to inhibit Notch activity in cancer treatment were developed. Inhibition of the aberrant Notch signaling pathway results in decreased tumor size, metastasis, and relapse in both *in vivo* and *in vitro* studies [6]. Inhibition of enzymatic activity by gamma-secretase inhibitors (GSI), which prevent the release of NICD, has shown successful clinical outcomes in treating several cancer types as a single agent and combined with standard chemotherapeutics [7, 8]. Dual antiplatelet therapy (DAPT) is an FDA-approved GSI that inhibits the cleavage of NICD and its release into the cytoplasm. DAPT showed successful clinical outcomes in treating various diseases, including breast cancer [9]. Considering treatment strategies are limited by the drug resistance phenomenon, the success of DAPT in breast cancer treatments relies on understanding possible resistance mechanisms against DAPT, which remains unknown. This study provides a perspective on potential resistance mechanisms against DAPT treatment in MCF-7 breast cancer cells.

Materials and methods

Cell culture and generation of resistant cell line

MCF-7 (ATCC HTB22) breast cancer cells were obtained from ATCC. The cells were cultured in DMEM (Sigma) containing 1% Penicillin/Streptomycin (Thermo) and 10% fetal bovine serum (Biological Industries) at 37 °C in 5% CO₂ incubation conditions. When they reached the confluency of 80–90%, cells were washed with phosphate buffer saline (PBS) and trypsinized (0.05%) for further passaging. A DAPT-resistant cell line was generated according to McDermott et al.'s published protocol [10]. Briefly, cells were treated with gradually increasing doses of DAPT (ADOOQ) (Figure 1A), from half of the IC₅₀ value (IC₂₅) to a four-fold IC₅₀ value (IC₂₀₀). Cells were plated into six-well plates, and 24 h later, the drug treatment started. After reaching 80–90% of confluency, approximately in ten days, the drug was washed away, and cells were maintained in a drug-free medium for twenty-four hours. Then, the cells were visualized under the light microscope for

morphological analysis, flash-frozen for mRNA expression analysis, and cryofreezed for further experiments. Each dose exposure was repeated twice. DAPT's solvent, Dimethyl sulfoxide (DMSO), was included as the control (Figure 1B).

Viability assay

MTT cell viability assay was used to determine the IC₅₀ dose for DAPT and to confirm the resistance of the treated cells. Cells were plated into 48-well plates and treated with increasing doses of DAPT (from 1 nM to 500 μM) or respective solvent control (DMSO) for 24 h. Then cells were treated with 5 mg/mL of 3-(4,5-Dimethylthiazol-2-yl)-2,5-Diphenyltetrazolium Bromide (Amnesco) for 4 h, followed by dissolving of tetrazolium salts in DMSO. The absorbance values were measured at 570 nm and 650 nm in a microtiter plate reader (Thermo Scientific Multiskan Spectrum). Each independent experimental setup was replicated at least three times and normalized to the control group.

Wound healing and circularity analysis

The cells (7.5×10^5 cells per well) were grown in monolayer in 24-well plates. Twenty-four hours later, cells were treated with 5 μg/ml Mitomycin C (Santa Cruz) at 37 °C for 3 h. Then the medium was removed, and a wound was generated with a sterile 10 μL pipette tip. Following a wash with PBS, cells were monitored in 500 μL of fresh serum-free medium per well. The wound was monitored at three different positions per well and imaged in 1 h intervals for 24 h using a Leica SP8 microscope at 4x magnification. Data are represented as the means and ± standard deviation (SD) of three independent experiments, graphed using Graphpad PRISM 8. The cells (1×10^4 cells per well) were plated onto 6-well plates for morphological analysis. After 24 h, phase contrast images were taken at 20x magnification using Leica DMI8 confocal microscope. The images were analyzed with Image J's circularity testing with the circularity baseline set to 4pi (area/perimeter²).

qRT-PCR

1 μg of total RNA, isolated with PureLink RNA Mini isolation kit (Invitrogen), was used to synthesize cDNA using the RevertAid First Strand cDNA Synthesis Kit (Fermentas). The qRT-PCR reaction was carried out on LightCycler 96 Real-Time PCR detection system (Roche) with Maxima SYBR Green qPCR Master Mix (Fermentas). The comparative delta-delta Ct method was applied, and TATA box-binding protein (TBP) expression was used for normalization. PCR reactions for each gene were repeated three times. The primer sequences are as follows: NOTCH1 CACTGCGAGGTCAACACAGA, GCACACTCGTCCACATCGTA; NOTCH2 TGTGCTCAAATCCATGCCT, ATGGTACACCGCTGACCTTG; NOTCH3 GCAGCGATGGAATGGGTTTC, CTGCCAGGTGGTGAGATA; NOTCH4 TTCCACTGTCTCCTGCCAGAA, HES1: AACACGACACCGGATAACC, TCAGCTGGCTCAGACTTTCA; HES5 ACATCCTGGAGATGGCTGTC, TAGTCCTGGTGCAGGCTCTT; HEY2 AAGATGCTTCAGGCAACAGG, GCACTCTCGGAATCCTATGC; E-Cadherin CAGCAGTACACAGCCCTAA, GGTATGGGGCGTGTGCATT; ZO-1: ATGGAGAAACAGCTATATGGA,

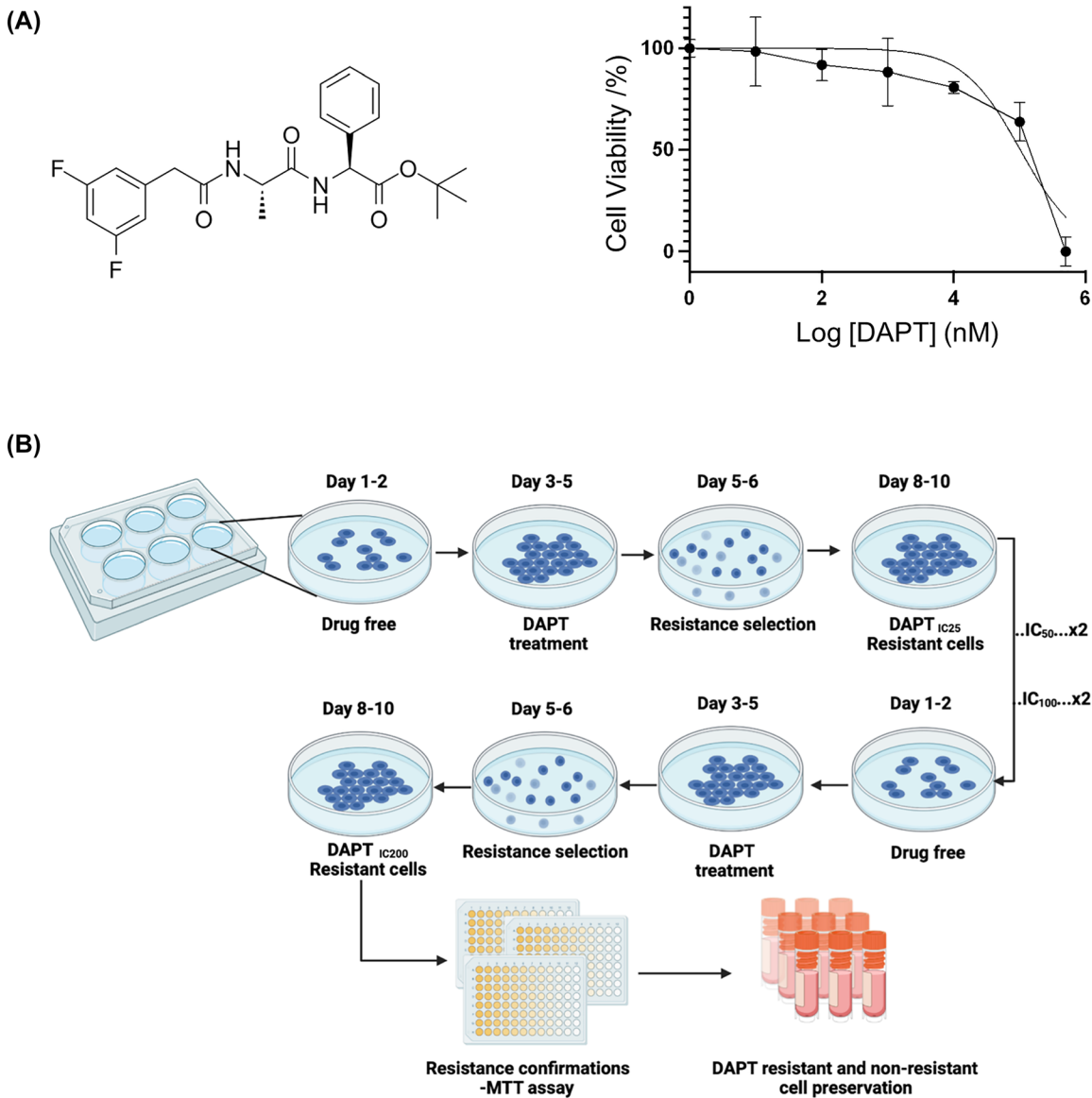


Figure 1: The experimental strategy to generate DAPT-resistant MCF-7 cells. (A) DAPT structure is shown on the left. IC_{50} curve for MCF-7 cells treated with DAPT is on the right. Cell viability percentage was plotted against the DAPT concentrations on a logarithmic scale. Data represent the means and \pm SD of two independent experiments and three measurements. (B) The schematic explanation of the protocol used to generate DAPT-resistant cells is shown. Each DAPT treatment was repeated a minimum of twice, along with DMSO controls. Cells were then preserved for further analysis. Viability changes of DAPT-resistant cells were confirmed with MTT assay.

CCAAATCCAAATCCAGGAGCC; N-Cadherin: CCTCCAGAGTTTACTGCCATGAC, GTAGGATCTCCGCACTGATT; SNAIL1 CTAGGCCCTGGCTGTACAA, TGTGGAGCAGGGACATTCG; SNAIL2 CTCTCATCTTTGGGGCGAG, TTCAATGGCATGGGGGTCTG; TBP TAGAAGGCCTTGTGCTCACC, TCTGCTCTGACTTTAGCACCTG.

Statistical analysis

One-way ANOVA was used for the statistical analysis of the circularity. Two-tailed paired t-test was used to assess the statistical significance of viability, qRT-PCR, and wound healing analyses.

Results

MCF-7 breast cancer cells undergo morphological changes upon acquired resistance to DAPT

First, to determine the half-maximal dose (IC_{50}) of the breast cancer cell line, MCF-7, we applied gradually increasing doses of DAPT from 1 nM to 500 μ M for 24 h. Then, we

analyzed viability by MTT assay and calculated the IC_{50} value using GraphPadPrism normalized inhibition response tool as $18.17 \mu\text{M}$ (Figure 1A). To model acquired resistance, we treated MCF-7 cells with gradually increasing doses of DAPT, from half the value (IC_{25}) up to four times the value (IC_{200}) of IC_{50} [10]. Briefly, 24 h after plating the cells in a drug-free medium, we started the treatment with IC_{25} of DAPT or an equal amount of DMSO as control. We refreshed the medium with DAPT every 48 h. After the cells reached 80–90% of confluency, we passaged the cells to a fresh plate and repeated the same protocol applying the same dose, IC_{25} , for the second round. Then, we transferred the cells to a fresh plate in a drug-free medium, and the same protocol was followed with the next dose, which was two times higher than the previous one (Figure 1B). In the end, we obtained MCF-7 cells that can grow to 90% confluency in the presence of IC_{200} of DAPT, which we will refer to as MCF-7-R from now on (Figure 2A). MCF-7 cells, which were treated with the respective volumes of DMSO throughout the procedure, were generated as the control (MCF-7-C). The growth rate of MCF-7-R was not significantly different from the control MCF-7-C cells (Figure 2B).

MCF-7-R cells showed morphological changes. In contrast to the control MCF-7-C cells, which have an epithelial-like phenotype, MCF-7-R cells acquired a more elongated mesenchymal-like phenotype (Figure 2A, left panels). To analyze the changes in the morphology, cells were plated at a lower density and visualized with higher magnification (Figure 3A). The mean circularity of the control cells was 0.88, while it was reduced to 0.61 in MCF-7-R cells, representing a more elongated shape (Figure 3B). Overall, the data showed that MCF-7 cells resistant to IC_{200} DAPT acquired a more mesenchymal morphology.

DAPT-resistant MCF-7 cells exhibit increased migration

Mesenchymal morphology is often associated with increased migration, a common trait of invasive and metastatic tumors. Drug resistance is also correlated with mesenchymal characteristics [3]. Thus, we analyzed whether MCF-7-R cells had an increased migration capacity using a wound healing assay. While only 13.2% of the open wound was closed by the control MCF-7-C cells, MCF-7-R cells reduced the gap by 51.1% in 20 h (Figure 4A and B), indicating a more migratory phenotype in correlation with the mesenchymal morphology.

DAPT-resistant MCF-7 cells regulate expression levels of notch pathway components and epithelial-mesenchymal transition markers

The Notch signaling pathway regulates multiple downstream targets [11]. To gain a more comprehensive insight into the mechanism behind the resistance, mRNA expression profiles of Notch receptors and common downstream targets were analyzed by quantitative qRT-PCR. In MCF-7-R cells, mRNA expression of Notch receptors NOTCH1 and NOTCH2 was downregulated by 50% and 60%, respectively (Figure 5A). On the other hand, NOTCH3 was upregulated by 2-fold, and NOTCH 4 did not change (Figure 5A). Notch target genes HES5 and HEY1 were upregulated by 1.8-fold, while HES1 was decreased by 50% (Figure 5B). Two epithelial markers showed an opposite trend that E-Cadherin was increased by 1.3-fold, while ZO-1 was decreased by 50%

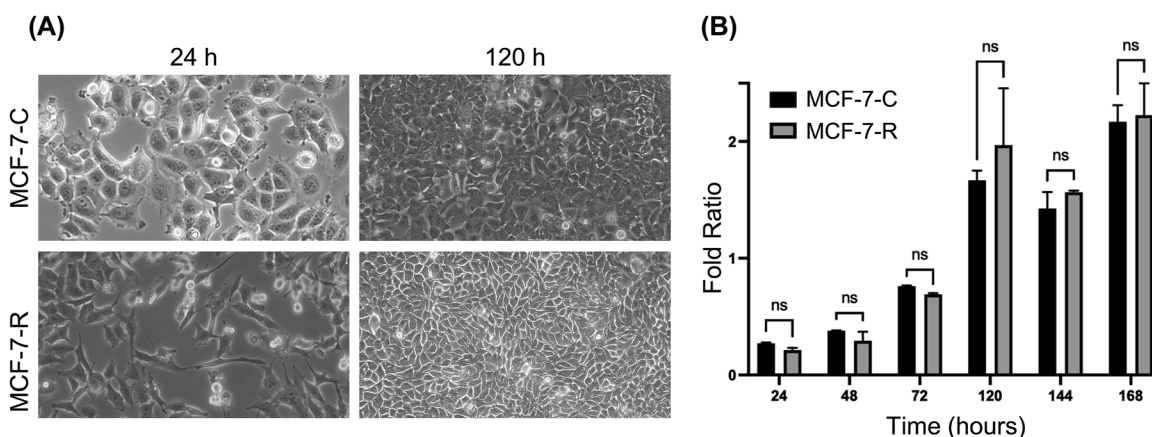


Figure 2: DAPT resistance induces morphological changes in MCF-7 cells. (A) Light microscopy images of MCF-7 cells resistant to IC_{200} DAPT treatment (MCF-7-R) and DMSO-treated control cells (MCF-7-C) were taken at 24 h and 120 h after DAPT and DMSO treatments, respectively. (Scale bar: $50 \mu\text{m}$). (B) Viability of MCF-7-R and MCF-7-C cells cultured in drug-free media at different time points. Data represents the means and \pm SD of two independent experiments (ns: not significant).

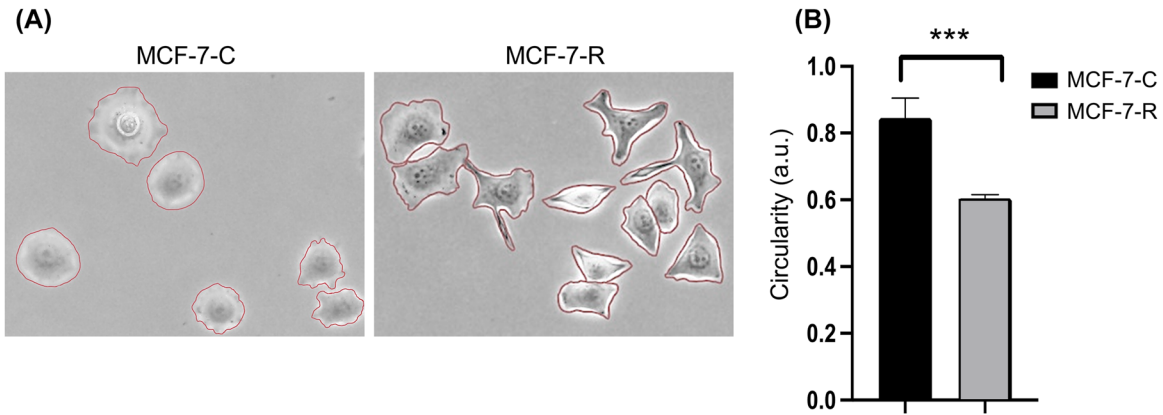


Figure 3: Circularity analysis of DAPT resistant and control cells. (A) Representative phase-contrast images of MCF-7-C and MCF-7-R cells plated in a drug-free medium. Red outlines representing the cell borders were used to calculate circularity. (Scale bar, 50 μm). (B) The circularity values (a.u.) of control and resistant cells are shown. Data represent the means and \pm SD of randomly selected 200 cells (***) $p < 0.001$.

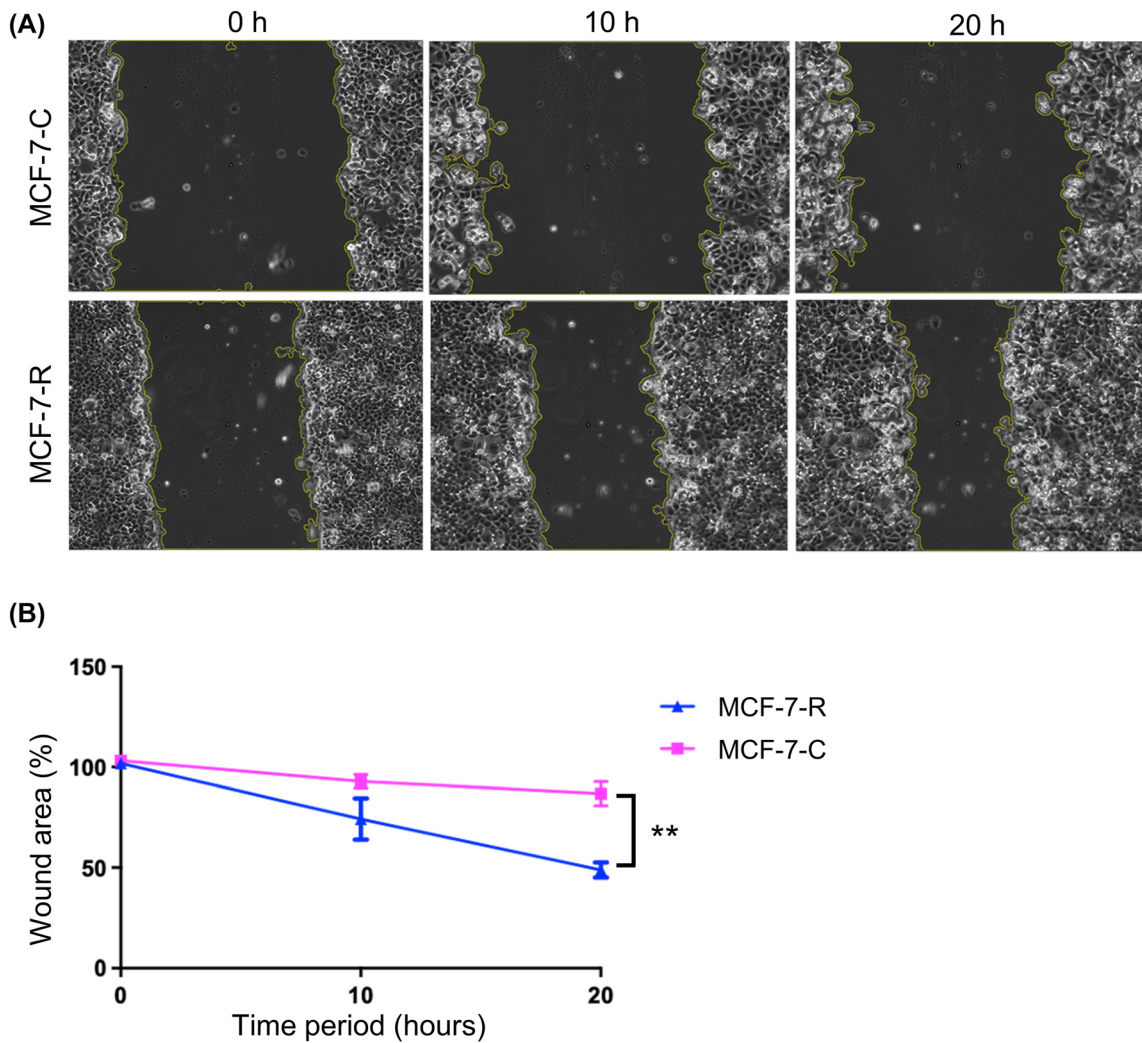


Figure 4: DAPT-resistant MCF-7 cells have increased migration capacity. (A) Time-lapse microscopy images of wound closure of MCF-7-C and MCF-7-R cells 0, 10, and 20 h after the wound formation. Yellow lines indicate the wound area. (Scale bar: 100 μm). (B) Percentage of open wound area in control and resistant cells. Data represent the means and \pm SD of three independent experiments (**) $p < 0.01$.

(Figure 5C). On the contrary, mRNA expressions of epithelial-mesenchymal transition (EMT) regulator SNAIL2 and mesenchymal marker N-Cadherin were increased by two- and 3-fold, respectively. In contrast, another EMT regulator, SNAIL1, was not changed in MCF-7-R cells (Figure 5D). Dysregulated downstream targets of Notch signaling and EMT markers propose a potential resistance mechanism of MCF-7 cells against DAPT.

Discussion

The Notch signaling pathway is activated by gamma-secretase complex-mediated cleavage upon receptor-ligand interaction [4]. DAPT is used to inhibit gamma-secretase complex and downregulate Notch signaling activity and was effective as an anti-neoplastic drug to treat several cancers, including breast cancer [12]. Its cytotoxic potential adheres vulnerable to possible resistance phenomena, which remains unknown. In this study, possible routes to DAPT resistance in MCF-7 breast cancer cells were investigated. MCF-7 is an epithelial breast cancer cell line positive for

estrogen and progesterone receptors. MCF-7 cells acquire resistance against hormone therapies due to the over-activated Notch signaling pathway. Furthermore, gamma-secretase inhibitor (GSI) therapies, including DAPT, increased the success of chemotherapies overall [5, 12, 13].

In MCF-7 cells, the half-maximal toxic dose of DAPT was observed at 18.17 μ M, reflecting a moderate intrinsic or acquired resistance. Various strategies to obtain resistance against anti-neoplastic drugs were previously investigated, and a gradual increase in the doses starting with IC_{50} showed the most successful outcome [10]. Here, we obtained MCF-7-R cells, which survive under IC_{200} DAPT treatment. This value exceeds the two-fold increase from IC_{50} that is accepted as the minimum dose the cells should survive to be considered resistant [10].

Cancer cells endure constant morphological and molecular changes to tolerate anti-neoplastic drug treatments. Phenotypical changes in cancer cells escalate migration and invasion, which are associated with drug resistance. Accordingly, the most striking observation in the DAPT-resistant MCF-7-R cells was the morphological shift towards a mesenchymal phenotype, accompanied by an increase in migratory

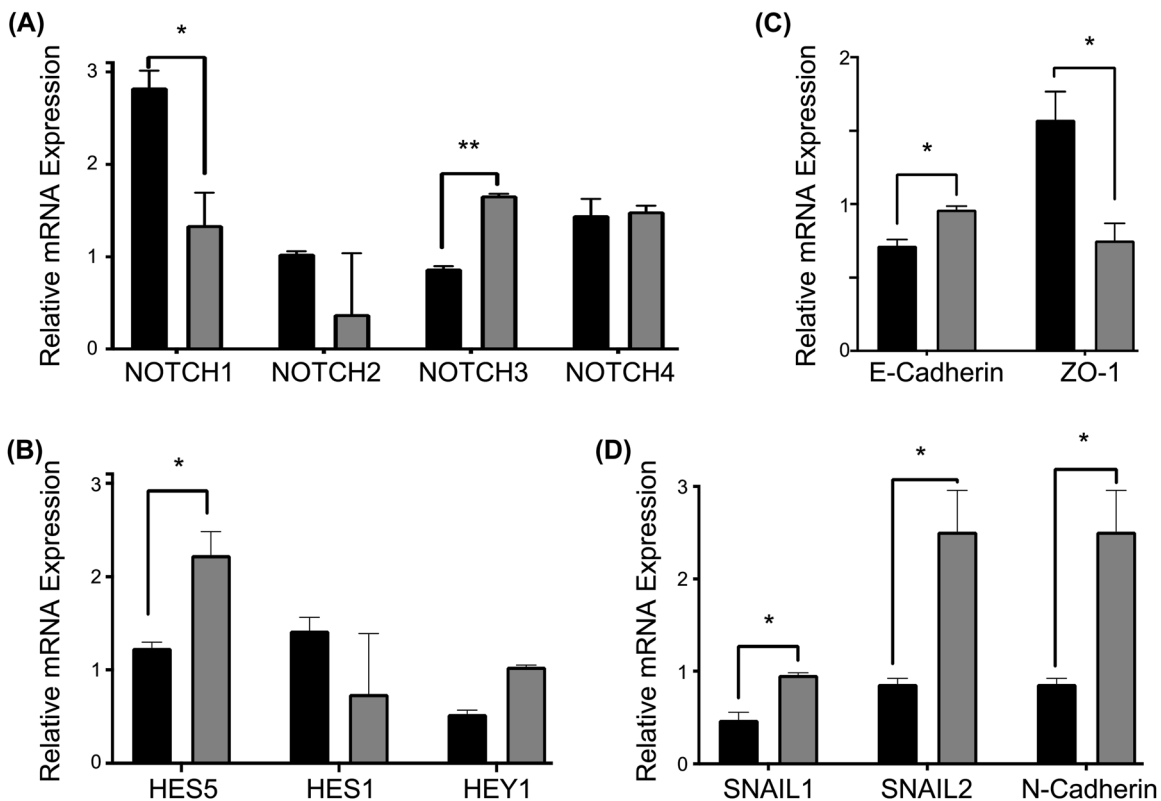


Figure 5: Expression analysis of notch pathway components and EMT markers. mRNA expression levels of (A) notch receptors (NOTCH 1,2,3 and 4), (B) notch pathway target genes (HES5, HES1, HEY1), (C) epithelial markers (E-cadherin, ZO-1), and (D) mesenchymal markers (SNAIL2, N-cadherin, and SNAIL1) of MCF-7-C and MCF-7-R cells are shown. Data represent the means and \pm SD of three independent experiments (ns: not significant, * p <0.05, ** p <0.01, *** p <0.001).

behavior. Alterations in the strictly balanced metabolism urge cells to undergo morphological and behavioral changes via epithelial-mesenchymal transition (EMT) [14]. Thus, we investigated whether EMT might explain the differences in MCF-7-R cells. In agreement with the activation of an EMT program, we observed an increase in EMT regulator SNAIL-2 and mesenchymal marker N-Cadherin, while an epithelial marker ZO-1 decreased. ZO-1 downregulation reflects metastatic behaviors and drug resistance [15, 16]. In addition to its role in EMT, SNAI2 regulates diverse functions in development and disease, including cancer, and is regulated by Notch signaling [17–19]. The two other markers, epithelial marker E-Cadherin, and EMT regulator SNAI1, were not changed in MCF-7-R cells, which could be explained by partial EMT or the existence of transitional states during EMT. The degree of EMT shift is cell- and context-dependent, which rarely exhibits a fully differentiated mesenchymal character [20]. Collectively, our results support the literature in which EMT-like transitions are potential targets of resistance to multiple anti-neoplastic drugs. Possible DAPT resistance mechanisms could rely on EMT, which has pleiotropic functions in cancer, such as favoring the migratory and invasive behavior, acquisition of stem-cell-like characteristics, and immune suppression in addition to drug resistance [21, 22].

Aberrant expression of Notch receptors is correlated with poor prognosis and recurrence in cancers and is suggested as a potential cancer biomarker. DAPT-resistant MCF-7 cells had reduced NOTCH1 receptor and HES1 target gene, while NOTCH3 receptor, HES5, and HEY1 target genes were upregulated. Aberrant expression of NOTCH1 induces stemness, metastasis, and cancer recurrence in T-cell acute lymphoblastic leukemia, ovarian, breast, colorectal, gastric, and lung cancer [23–27]. NOTCH2 functions as a tumor suppressor in laryngeal squamous cell carcinoma and breast and gastric cancers [28, 29]. Dysregulated expressions of NOTCH3 and NOTCH4 induce tumorigenesis and drug resistance in breast and colorectal cancer [30, 31]. Upregulation of NOTCH3 might point to a compensation mechanism to overcome the effects of GSI treatment. Notch downstream targets HES5 and HEY1 play an oncogenic role and stimulate EMT transition, invasion, metastasis, cancer stemness, and multidrug resistance, whereas HES1 has a tumor-suppressor role in hepatocarcinogenesis, nasopharyngeal carcinoma and salivary adenoid cystic carcinoma cells [32–34]. Although we cannot exclude a Notch-independent mechanism, SNAI2, HES5, and HEY1 induction upon compensatory activation of Notch signaling over NOTCH3 might trigger an EMT program in MCF-7-R cells.

In conclusion, we showed that compensatory activation of Notch signaling and EMT induction could be potential

resistance mechanisms against DAPT treatment in MCF-7 breast cancer cells. Further investigation of molecular profiles concerning the traits of aggressive tumors will increase our understanding of possible resistance mechanisms against GSI. Currently, GSI treatments receive interest in both pre-clinical and clinical stages and focusing on managing potential resistance responses against GSI will prolong success in cancer treatment.

Research funding: This work was supported by the Izmir Institute of Technology (IYTE0221).

Author contributions: O.Y.O. conceived the project and acquired the funding; K.T. performed the experiments and analyzed the data; K.T. and O.Y.O. wrote the manuscript. All authors have accepted responsibility for the entire content of this manuscript and approved its submission.

Competing interests: Authors state no conflict of interest.

Informed consent: Not applicable.

Ethical approval: Not applicable.

References

- Alfarouk KO, Stock CM, Taylor S, Walsh M, Muddathir AK, Verduzco D, et al. Resistance to cancer chemotherapy: failure in drug response from ADME to P-gp. *Cancer Cell Int* 2015;15:71.
- Colleoni M, Sun Z, Price KN, Karlsson P, Forbes JF, Thürlimann B, et al. Annual hazard rates of recurrence for breast cancer during 24 years of follow-up: results from the international breast cancer study group trials I to V. *J Clin Oncol* 2016;34:927–35.
- Shibue T, Weinberg RA. EMT, CSCs, and drug resistance: the mechanistic link and clinical implications. *Nat Rev Clin Oncol* 2017;14: 611–29.
- Bray SJ. Notch signalling: a simple pathway becomes complex. *Nat Rev Mol Cell Biol* 2006;7:678–89.
- Edwards A, Brennan K. Notch signalling in breast development and cancer. *Front Cell Dev Biol* 2021;9:692173.
- Brennan K, Clarke RB. Combining notch inhibition with current therapies for breast cancer treatment. *Ther Adv Med Oncol* 2013;5: 17–24.
- Takebe N, Nguyen D, Yang SX. Targeting notch signaling pathway in cancer: clinical development advances and challenges. *Pharmacol Ther* 2013;141:140–9.
- Tamagnone L, Zacchigna S, Rehman M. Taming the notch transcriptional regulator for cancer therapy. *Molecules* 2018;23:431
- Feng J, Wang J, Liu Q, Li J, Zhang Q, Zhuang Z, et al. DAPT, a γ -secretase inhibitor, suppresses tumorigenesis, and progression of growth hormone-producing adenomas by targeting notch signaling. *Front Oncol* 2019;9:809.
- McDermott M, Eustace AJ, Busschots S, Breen L, Crown J, Clynes M, et al. In vitro development of chemotherapy and targeted therapy drug-resistant cancer cell lines: a practical guide with case studies. *Front Oncol* 2014;4:40.
- Kar R, Jha NK, Jha SK, Sharma A, Dholpuria S, Asthana N, et al. A “NOTCH” deeper into the Epithelial-to-Mesenchymal Transition (EMT) program in breast cancer. *Genes* 2019;10:961.

12. Moore G, Annett S, McClements L, Robson T. Top notch targeting strategies in cancer: a detailed overview of recent insights and current perspectives. *Cells* 2020;9:1503.
13. Devarajan E, Chen J, Multani A, Pathak S, Sahin A, Mehta K. Human breast cancer MCF-7 cell line contains inherently drug-resistant subclones with distinct genotypic and phenotypic features. *Int J Oncol* 2002;20:913–20.
14. Wang J, Wei Q, Wang X, Tang S, Liu H, Zhang F, et al. Transition to resistance: an unexpected role of the EMT in cancer chemoresistance. *Genes Dis* 2016;3:3–6.
15. Kalluri R, Weinberg RA. The basics of epithelial-mesenchymal transition. *J Clin Invest* 2010;120:1786.
16. Polette M, Mestdagt M, Bindels S, Nawrocki-Raby B, Hunziker W, Foidart JM, et al. β -Catenin and ZO-1: shuttle molecules involved in tumor invasion-associated epithelial-mesenchymal transition processes. *Cells Tissues Organs* 2007;185:61–5.
17. Barrallo-Gimeno A, Nieto MA. The Snail genes as inducers of cell movement and survival: implications in development and cancer. *Development* 2005;132:3151–61.
18. Casas E, Kim J, Bendesky A, Ohno-Machado L, Wolfe CJ, Yang J. Snail2 is an essential mediator of Twist1-induced epithelial mesenchymal transition and metastasis. *Cancer Res* 2011;71:245–54.
19. Zhou W, Gross KM, Kuperwasser C. Molecular regulation of Snai2 in development and disease. *J Cell Sci* 2019;132:1–12.
20. Nieto MA, Huang RYJ, Jackson RA, Thiery JP. EMT: 2016. *Cell* 2016;166:21–45.
21. Liao TT, Yang MH. Revisiting epithelial-mesenchymal transition in cancer metastasis: the connection between epithelial plasticity and stemness. *Mol Oncol* 2017;11:792–804.
22. Varga J, Greten FR. Cell plasticity in epithelial homeostasis and tumorigenesis. *Nat Cell Biol* 2017;19:1133–41.
23. Bajaj J, Maliekal TT, Vivien E, Pattabiraman C, Srivastava S, Krishnamurthy H, et al. Notch signaling in CD66+ cells drives the progression of human cervical cancers. *Cancer Res* 2011;71:4888–97.
24. Bauer L, Takacs A, Slotta-Huspenina J, Langer R, Becker K, Novotny A, et al. Clinical significance of NOTCH1 and NOTCH2 expression in gastric carcinomas: an immunohistochemical study. *Front Oncol* 2015;5:94.
25. Deep G, Agarwal R. Antimetastatic efficacy of silibinin: molecular mechanisms and therapeutic potential against cancer. *Cancer Metastasis Rev* 2010;29:447–63.
26. Purow BW, Haque RM, Noel MW, Su Q, Burdick MJ, Lee J, et al. Expression of notch-1 and its ligands, delta-like-1 and jagged-1, is critical for glioma cell survival and proliferation. *Cancer Res* 2005;65:2353–63.
27. Wang Z, Banerjee S, Li Y, Rahman KM, Zhang Y, Sarkar FH. Down-regulation of notch-1 inhibits invasion by inactivation of nuclear factor-kappaB, vascular endothelial growth factor, and matrix metalloproteinase-9 in pancreatic cancer cells. *Cancer Res* 2006;66:2778–84.
28. Capulli M, Hristova D, Valbret Z, Carys K, Arjan R, Maurizi A, et al. Notch2 pathway mediates breast cancer cellular dormancy and mobilisation in bone and contributes to haematopoietic stem cell mimicry. *Br J Cancer* 2019;121:157–71.
29. Zou Y, Fang F, Ding YJ, Dai MY, Yi X, Chen C, et al. Notch 2 signaling contributes to cell growth, anti-apoptosis and metastasis in laryngeal squamous cell carcinoma. *Mol Med Rep* 2016;14:3517–24.
30. Koch U, Radtke F. A third Notch in colorectal cancer progression and metastasis. *J Exp Med* 2020;217:e20201017.
31. Xiu M, Wang Y, Li B, Wang X, Xiao F, Chen S, et al. The role of Notch3 signaling in cancer stemness and chemoresistance: molecular mechanisms and targeting strategies. *Front Mol Biosci* 2021;8:694141.
32. Liu ZH, Dai XM, Du B. Hes1: a key role in stemness, metastasis and multidrug resistance. *Cancer Biol Ther* 2015;16:353–9.
33. Luiken S, Fraas A, Bieg M, Sugiyanto R, Goeppert B, Singer S, et al. NOTCH target gene HES5 mediates oncogenic and tumor suppressive functions in hepatocarcinogenesis. *Oncogene* 2020;39:3128–44.
34. Xie J, Lin LS, Huang XY, Gan RH, Ding LC, Su BH, et al. The NOTCH1-HEY1 pathway regulates self-renewal and epithelial-mesenchymal transition of salivary adenoid cystic carcinoma cells. *Int J Biol Sci* 2020;16:598–610.